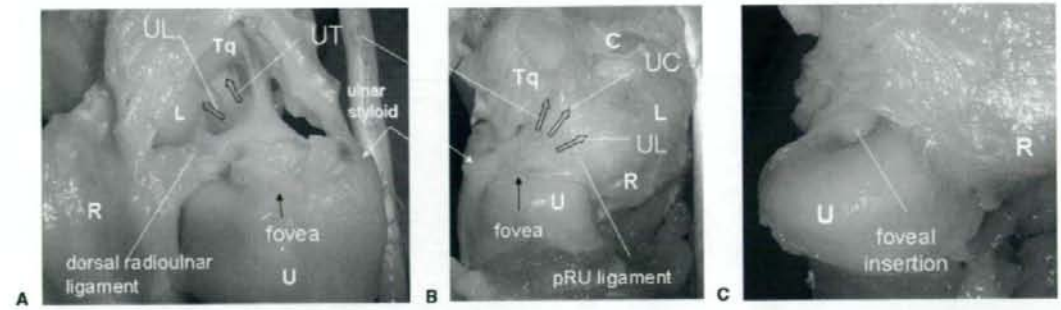

FIGURE 1: Anatomy of the ulnocarpal ligaments in a right cadaver wrist. A Dorsal view, B and C palmar views (C in supination). The ulnotriquetral (UT), ulnocapitate (UC), and ulnolunate (UL) ligaments originate together at the fovea of the ulnar head and the base of the ulnar styloid. These ligaments, along with the palmar radioulnar (pRU) ligament, extend distally like a fan in the coronal plane and insert at the palmar aspects of the triquetrum (Tq), capitate (C), and lunate (L). The joint capsule and the extensor tendons are removed. The ulnocapitate ligament is not visible from the dorsal view. R, radius; U, ulna.

THE DISTAL ULNA and the triangular fibrocartilage complex (TFCC) attached to it are essential in the coordination of the distal radioulnar joint and the ulnocarpal joint.[1] The distal radioulnar ligament and the ulnocarpal ligament are both essential ligamentous components of the TFCC. They originate together at the fovea of the ulnar head and at the base of the ulnar styloid process (Fig. 1).[1,2] A recent biomechanical study has shown that the foveal insertion has a greater effect on stability than does the styloid insertion.[3] It has been suggested that the reason for this is the closer relationship of the foveal insertion to the rotational axis of the forearm that runs through the foveal region.[4]

The foveal insertion of the TFCC is a key stabilizer of the distal radioulnar joint.[3] Thus, when this insertion fails to heal adequately after injury, distal radioulnar joint instability may develop, resulting in pain, decreased grip strength, and mechanical symptoms. Based on this concept, clinicians have recently advocated that patients with ulnar detachment of the TFCC require repair of the TFCC not to the capsule[5] but to the fovea.[6-8]

Despite the recognition of foveal lesions and their effects on distal radioulnar joint stability, the mechanism of injury in a foveal tear remains unclear. Only a few biomechanical studies have examined the mechanism of injury of the TFCC foveal tear.[9,10] It has been suggested that traumatic foveal lesions result from forces generated by forearm hyper-rotation, distal radioulnar joint distraction, wrist axial loading, or some combination of these factors.[8,11] However, neither extreme rotational forces[9] nor the axial load during injury[10] alone can reproduce a traumatic foveal lesion.

A few biomechanical investigations of the function of the ulnocarpal ligament suggest that the ulnocarpal ligament has an important role in stabilizing the ulnocarpal joint[12,13]; however, there has been little or no discussion of the relationship between the ulnocarpal ligament and the foveal triangular fibrocartilage complex tear. Moreover, all of the current information regarding the function of the ulnocarpal ligament has been acquired in cadaver model studies using invasive procedures. Such *in vitro* experiments cannot completely reproduce the physical muscular force that is exerted across the wrist joint *in vivo*. This limitation could alter the normal kinematics of the ligaments. Recently, researchers have been able to measure *in vivo* kinematics of the human joint[14-16] and ligament length[17] using noninvasive techniques.

The fovea of the ulnar head is the primary attachment site for both the distal radioulnar and ulnocarpal ligaments, so that both are affected simultaneously by traumatic avulsion of the TFCC from its ulnar attachment. We therefore designed this study to investigate changes in the length of the ulnocarpal ligaments during various radiocarpal motions using *in vivo* 3-dimensional motion analysis. The purpose of this study was to determine the type of wrist radiocarpal motion that makes the ulnocarpal ligament taut and can cause foveal avulsion if it is excessive.

MATERIALS AND METHODS

The *in vivo* 3-dimensional kinematics of the wrist joint in a total of 15 right wrists of healthy volunteers was studied. Flexion–extension motion, radioulnar deviation, and the so-called dart-throwing motion were investigated in 5 volunteers each. The average age of the volunteers was 28 years (range, 20–32 years). There were 11 men and 4 women. All volunteers gave their written informed consent prior to inclusion in the study.

Magnetic resonance images were acquired using the same method as reported previously.[14,16] To immobilize the elbow and the wrist at a specific angle during each wrist motion, a special posture device, which has a grip bar and goniometers, was used. This device has 3 motion axes, all of which cross perpendicularly at the wrist joint and enable the wrist to move along any specific plane.

Magnetic resonance images were acquired in 7 positions during flexion–extension motion from 60° extension to 60° flexion in 20° increments, in 7 positions during radioulnar deviation from 20° radial deviation to 40° ulnar deviation in 10° increments, and in 5 positions during dart-throwing motion from 40° radial deviation–extension (radial extension) to 40° ulnar deviation–flexion (ulnar flexion) in 20° increments.

The contours of each bone were mapped from the magnetic resonance volume images. The 3-dimensional surface models of the bones were constructed using a software program (Virtual Place-M; AZE, Tokyo, Japan). The kinematic variables were calculated by registering the bone in one position and then comparing it in other positions. The volume registration technique was conducted using the same software program. The ulna, the radius, and all the carpal bones except the pisiform were registered, and the motion of each bone relative to the ulna was calculated. Three-dimensional animations of the motions of the radius, the carpus, and the ligaments with respect to the fixed ulna were created by using software that was developed in our laboratory (Orthopedics Viewer; Osaka University, Osaka, Japan).

We modeled 4 ligament paths consisting of the ulnotriquetral (UT), ulnolunate (UL), ulnocapitate (UC), and palmar radioulnar (pRU) ligaments. The origin and insertion of the ligament models investigated in this study were based on information from our own cadaver dissection and previous anatomical studies.[1,2,18] These points were located by comparing anatomic information and the bony geometry on the 3-dimensional bone model.

The UT, UC, and UL ligaments originate together at the fovea of the ulnar head and at the base of the ulnar styloid process (Figs. 1 and 2). These ligaments, along with the pRU ligament, extend distally like a fan in the coronal plane and insert at the palmar aspects of the triquetrum, capitate, and lunate. The UC ligament emerges from the fovea and courses across the anterior border of the triangular fibrocartilage and attaches into the anteromedial aspect of the capitate.[18] When the ulnocarpal ligament is inspected from the palmar side on cadaver specimens, the UT, UL, and UC ligaments

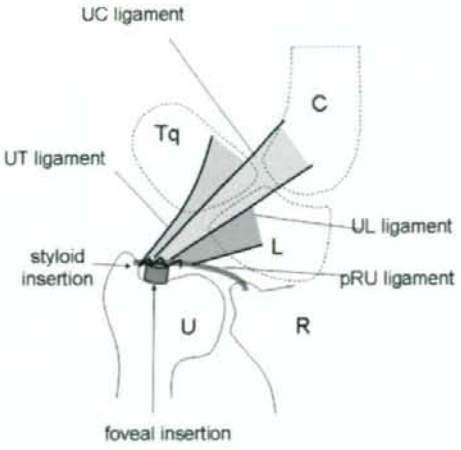

FIGURE 2: A schema of the ulnocarpal ligaments and the palmar radioulnar ligament viewed from the palmar side.

FIGURE 3: The fovea on a 3-dimensional model of the right ulna viewed from the palmar side.

are confluent but the UC ligament runs more superficial than the UT and UL ligaments. In this study, the origins of all ligaments were placed at the fovea of the ulnar head, which was determined as the deepest point of the distal surface of the ulnar head (Fig. 3).

The insertion of the UT ligament was placed at a point just ulnar to the lunotriquetral joint on the palmar tuberosity of the triquetrum. The insertion of the UL ligament was placed at a point just radial to the lunotriquetral joint on the palmar tuberosity of the lunate. The insertion of the UC ligament was placed at the proximal and ulnar corner of the palmar tuberosity of the capitate. The insertions of the pRU ligaments were placed at the ulnopalmar corner of the distal radius.

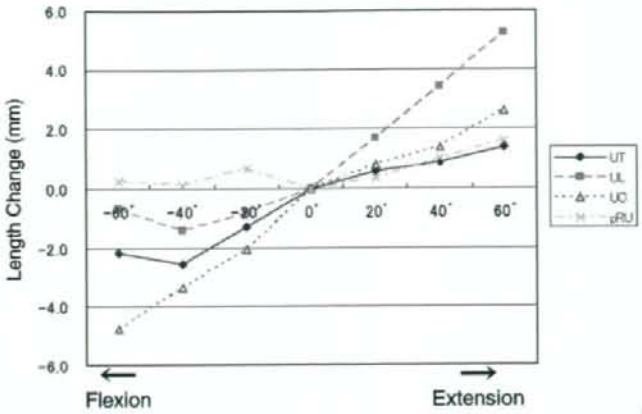

FIGURE 4: Change in the length of the 3 ulnocarpal ligaments and of the palmar radioulnar ligament during flexion–extension motion.

Based on the method proposed by Marai et al.,[17] these ligament models were calculated as the shortest paths in a 3-dimensional space that includes bone obstacles. The method to calculate the shortest paths takes into account the fact that the ligament does not go in a straight line from origin to insertion but detours around bony protrusions. Structural and material properties of the ligaments are not taken into account by this computer program. We calculated the 3-dimensional distance of the UT, UL, UC, and pRU ligaments during flexion–extension motion, radioulnar deviation, and dart-throwing motion.

All data are expressed as means ± standard deviation. Statistical analysis of differences was performed using Student's *t*-test. The significance level was $p < .05$.

RESULTS

Flexion–extension motion

From the wrist neutral position to extension, the length of the UT, UL, and UC ligaments increased by 1.4 mm ± 1.5 mm, 5.2 mm ± 1.6 mm, and 2.6 mm ± 0.5 mm, respectively (Fig. 4). From the wrist neutral position to flexion, the length of UT, UL, and UC ligaments decreased by 2.2 mm ± 1.5 mm, 0.7 mm ± 1.7 mm, and 4.8 mm ± 1.5 mm, respectively. The animations of the wrist joint from wrist flexion to extension showed that, as the triquetrum, lunate, and capitate rotate dorsally, the paths of the UT, UL, and UC ligaments gradually develop a detour toward the palmar side, because of a palmar protrusion of the proximal part of the triquetrum and lunate (Fig. 5). (The supplementary video can be viewed at the *Journal's* Web site, http://www.jhandsurg.org.) The degree of the palmar protrusion of the triquetrum in wrist extension appeared to be less than that of the lunate. The change in length of the pRU ligament was relatively small (1.6 mm ± 1.0 mm in extension, 0.2 mm ± 0.8 mm in flexion).

Radioulnar deviation

From the wrist neutral position to radial deviation, the length of the UT, UL, and UC ligaments increased by 1.1 mm ± 0.4 mm, 0.0 mm ± 0.5 mm, and 0.9 mm ± 0.8 mm, respectively (Fig. 6). From the wrist neutral position to ulnar deviation, the length of the UT and UC ligaments decreased by 1.1 mm ± 0.8 mm and 2.1 mm ± 2.0 mm, respectively, but that of the UL ligament increased by 2.3 mm ± 1.7 mm. The animations showed that, during radioulnar deviation, the UT and UC ligaments and the UL ligament showed reciprocal behavior with respect to each other (Fig. 7). (The supplementary video can be viewed at the *Journal's* Web site, http://www.jhandsurg.org.) During wrist ulnar deviation, the lunate rotated dorsally, which appeared to stretch the UL ligament. The triquetrum also rotated dorsally but shifted toward the ulnar head, which appeared to cancel the length increase of the UT ligament generated by dorsal rotation. The length of the pRU ligament changed minimally (0.3 mm ± 0.5 mm in radial deviation, 0.3 mm ± 0.3 mm in ulnar deviation).

Dart-throwing motion

From the wrist neutral position to radial extension, the length of the UT, UL, and UC ligaments increased by 3.0 mm ± 1.7 mm, 1.8 mm ± 1.7 mm, and 4.0 mm ±

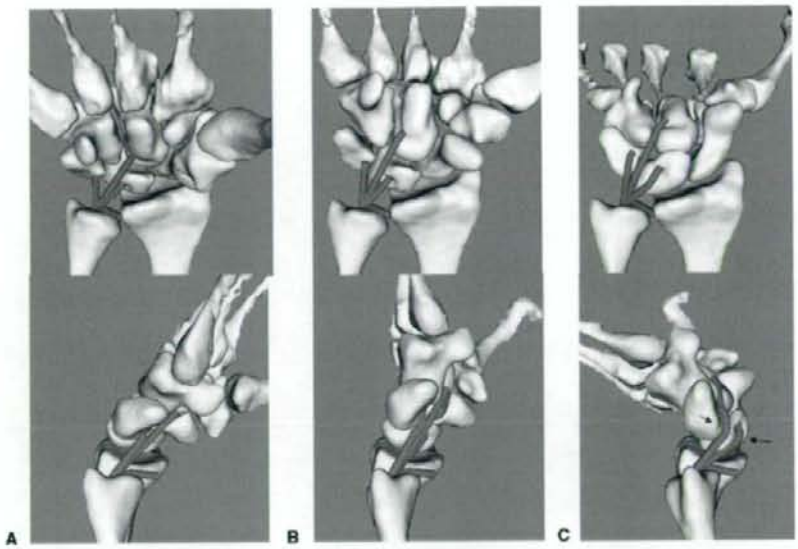

FIGURE 5: Three-dimensional ligament paths in wrist flexion **A**, neutral position **B**, and extension **C** during flexion–extension motion viewed from the palmar side and the ulnar side in a representative case. Note that, in wrist extension, the ligament paths detour toward the palmar side because of the palmar protrusion of the triquetrum and lunate (arrow). A video of a representative case may be viewed at the *Journal's* Web site, http://www.jhandsurg.org.

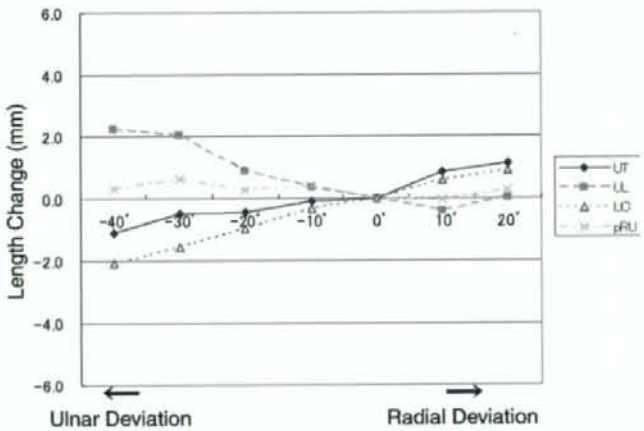

FIGURE 6: Change in the length of the 3 ulnocarpal ligaments and of the palmar radioulnar ligament during radioulnar deviation.

1.1 mm, respectively (Fig. 8). From the wrist neutral position to ulnar flexion, the length of the UT and UC ligaments decreased by 1.6 mm ± 0.5 mm and 2.2 mm ± 0.6 mm, respectively, but that of the UL ligament increased by 1.2 mm ± 1.1 mm. The animations showed that, in wrist radial extension, the capitate insertion of the UC ligament shifted to the radiodorsal direction, and palmar protrusion of the capitate head made the UC ligament detour toward the palmar side (Fig. 9). (The supplementary video can be viewed at the *Journal's* Web site, http://www.jhandsurg.org.) The animations also showed that the triquetrum shifted distally, whereas the lunate moved only slightly. The length of the pRU ligament changed little (0.5 mm ± 1.0 mm in radial extension, 1.2 mm ± 0.6 mm in ulnar flexion).

The length of the UT and UC ligaments increased the most in wrist radial extension, and the length of the

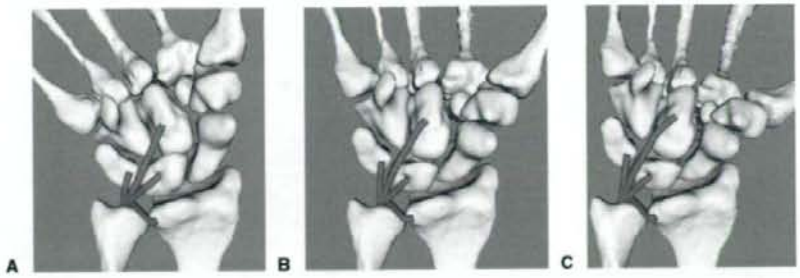

FIGURE 7: Three-dimensional ligament paths in **A** ulnar deviation, **B** neutral position, and **C** radial deviation during radioulnar deviation, viewed from the palmar side in a representative case. Note that the UT and UC ligaments and the UL ligament show reciprocal behavior with respect to each other. A video of a representative case may be viewed at the *Journal's* Web site, http://www.jhandsurg.org.

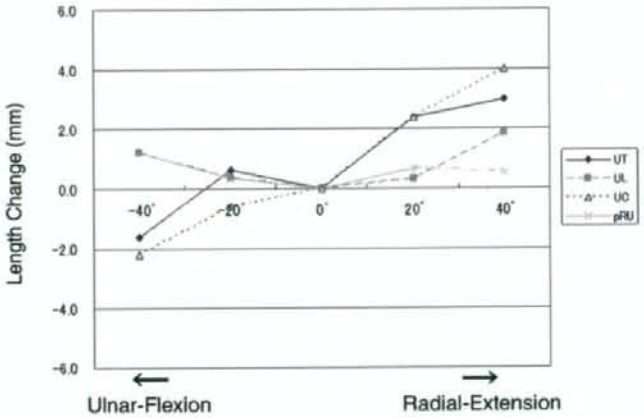

FIGURE 8: Change in the length of the 3 ulnocarpal ligaments and of the palmar radioulnar ligament during dart-throwing motion.

UL ligament increased the most in wrist extension. The changes in length of the UT ligament in wrist radial extension were significantly greater than in wrist extension or radial deviation ($p < .05$ and $p < .005$, respectively). The changes in length of the UC ligament in wrist radial extension were significantly greater than in wrist extension or radial deviation ($p < .05$ and $p < .005$, respectively). The changes in length of the UL ligament in wrist extension were significantly greater than in wrist radial extension ($p < .05$). The length of the pRU ligament did not change significantly in any motion.

DISCUSSION

The pathomechanics of a traumatic triangular fibrocartilage complex foveal tear are not yet well understood. Anatomically, the fovea of the ulnar head is the primary attachment site for both the distal radioulnar and ulnocarpal ligaments; therefore, both should be affected simultaneously in this type of injury. However, little attention has been directed toward the role that the ulnocarpal ligaments play in the pathomechanics of this injury. Therefore, this study investigated the type of wrist radiocarpal motion that makes the ulnocarpal ligament taut and that can cause foveal avulsion of the TFCC if the motion is excessive.

The present *in vivo* study has some limitations. The origin and insertion of the ligaments were determined based only on anatomic information; individual variances in ligamentous anatomy were not taken into account. Our method does not take into account the width or the material properties of the ligaments. Real ligaments seldom extend or contract, although in our videos the ligament models appear elastic (Videos may be viewed at the *Journal's* Web site, www.jhandsurg.org.). This fact may influence the interaction with

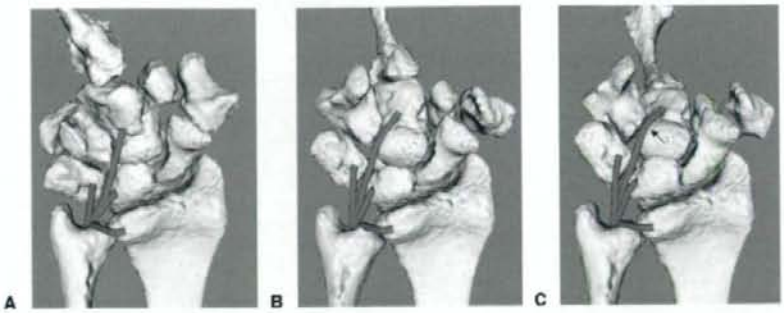

FIGURE 9: Three-dimensional ligament paths in **A** flexion, **B** neutral position, and **C** extension during dart-throwing motion, viewed from the palmar side in a representative case. The third metacarpals are shown, to indicate the global wrist position. Note that the capitate insertion of the UC ligament shifted to the radiodorsal direction, and palmar protrusion of the capitate head made the UC ligament detour toward the palmar side. A video of a representative case can be viewed at the *Journal's* Web site, http://www.jhandsurg.org.

neighboring soft tissues, such as the adjacent ligaments, the articular disk, and the meniscus homolog. Nonetheless, the animations of the ulnocarpal ligament paths that were created provided new visual information about the ligamentous kinematics and helped identify a potential mechanism for TFCC foveal tear.

There has been some confusion regarding the origin of the ulnocarpal ligament. When the ulnocarpal ligaments are inspected arthroscopically, their origin appears to be along the entire palmar extent of the triangular fibrocartilage complex. When inspected from the palmar side on cadaver specimens, however, the 3 fibers of the ulnocarpal ligaments are confluent and appear to converge into the fovea. We think that the ulnocarpal ligament that is seen arthroscopically is just a distal part of the ligaments, and that in fact the fibers of these ligaments extend proximally toward the fovea—although some fibers of the ligaments mingle with the palmar radioulnar ligament.

The function of the ulnocarpal ligament is not yet fully understood.[18,19] In particular, the ligamentous behavior during the dart-throwing motion has never been investigated. Weaver et al.[20] investigated the *in situ* tensions of the UL ligament in cadaver specimens and found that the tension of the UL ligament increased in ulnar deviation, supination, and extension. Wiesner et al.[21] applied progressive posteroanterior forces in the palmar direction to the carpus and found that the largest displacement was observed after the ulnar insertion of the ulnocarpal ligaments was sectioned. It has also been reported that the ulnocarpal ligaments can prevent abnormal radioulnar translations of the carpus.[12,13] All these findings suggest that the ulnocarpal ligaments have an important role in stabilizing the ulnocarpal joint.

We found that the greatest length increase of the UT and UC ligaments occurred with wrist radial extension during dart-throwing motion. It has been reported that midcarpal motion is substantial during dart-throwing motion,[16] and that the scaphoid and lunate move less.[15] Our animations in wrist radial extension showed that the capitate insertion of the UC ligament shifted distally, and that the UC ligament path developed a detour due to the palmar protrusion of the capitate head. The animations also showed that the triquetrum shifted distally without significant rotation, while the lunate seldom moved. These carpal movements that occur during wrist hyper-radial extension motion result in substantial strain to the UC and UT ligaments and on the foveal insertion of the TFCC. In comparison, the greatest length increase of the UL ligament was found in pure wrist extension. In the wrist extension animation, the palmar protrusion of the proximal portion of the lunate was greater than that of the triquetrum. This may explain why the length of the UL ligament increased more than the length of the UT ligament. In wrist extension, the UL ligament probably becomes taut and stretches the foveal insertion of the TFCC as well.

From wrist ulnar deviation to radial deviation, the length of the UT ligament increased, but the length of the UL ligament decreased. That is, during radioulnar deviation, the UT ligament and the UL ligament showed reciprocal behavior with respect to each other. We note that these 2 ligaments have an opposite function in terms of carpal stability during radioulnar deviation, even though, macroscopically, these 2 ligaments are often confluent and indistinguishable from each

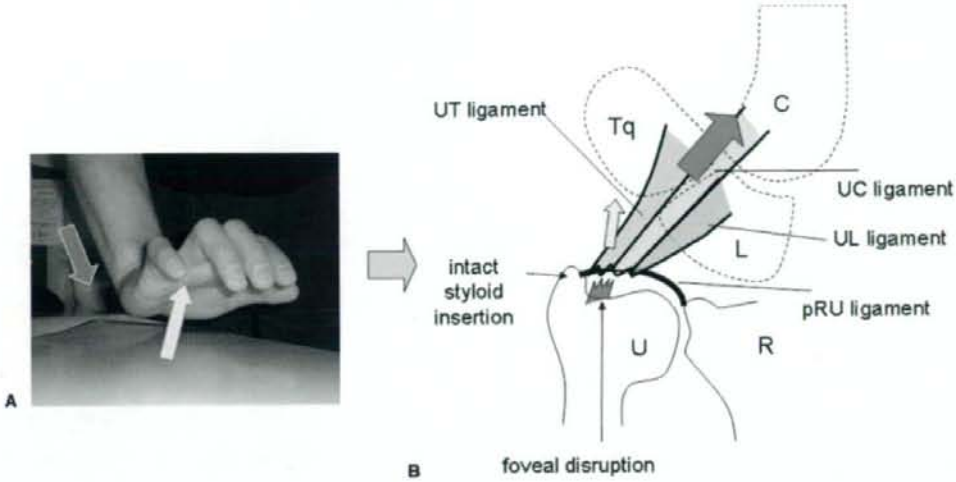

FIGURE 10: A Foveal disruption can result from a fall on the outstretched hand due to excessive traction of the ulnocarpal ligament in hyper-radial extension or extension of the wrist. The styloid insertion may be left intact. **B** The hypothesized mechanism of a triangular fibrocartilage complex foveal tear.

other.[18] It is possible that these 2 ligaments work together to provide a continuous and stable ulnar–radial–carpal motion throughout wrist radioulnar deviation.

The visualization of the pathomechanics of the TFCC tear may have been obscured by the relatively rigid prominence given to rotational injuries of the forearm; in fact, almost half of the reported cases of triangular fibrocartilage complex tears result from a fall on the outstretched hand.[6,7,22,23] For example, Hermansdorfer and Kleinman[6] reported 11 cases of peripheral triangular fibrocartilage complex tears, which included 5 cases caused by a fall. These facts strongly imply that forced wrist extension or radial extension, rather than forced pronosupination, may be a major factor in the pathomechanics of this type of injury (Fig. 10).

Based on the present findings, one possible injury mechanism of a triangular fibrocartilage complex foveal tear is excessive traction of the ulnocarpal ligament caused by wrist hyper-radial extension or hyperextension. However, this lesion does not result from forces generated only by simple wrist hyper-radial extension or hyperextension. Additional forces, such as axial loading or forearm rotation (or both), are probably required, at least to initiate the tear. Considering that the ulnocarpal ligament has another origin on the palmar aspect of the ulnar styloid,[2] which is eccentric from the center of forearm rotation (fovea), it is easily seen that the change in length of this fascicle would be increased by forearm supination. Strain of this fascicle during forearm supination may thus affect the tension of the foveal insertion.

This biomechanical study supports the hypothesis that one of the mechanisms of TFCC foveal tear can be excessive traction of the ulnocarpal ligament caused by a fall on the outstretched hand. Thus, to identify the exact location of the TFCC tear, clinical and radiographic examinations that pay particular attention to the ulnocarpal ligament lesion should be considered when dealing with patients who have ulnar wrist pain.

REFERENCES

1. Hagert CG. Current concepts of the functional anatomy of the distal radioulnar joint, including the ulnocarpal junction. In: Büchler U, ed. Wrist instability. London: Martin Dunitz, 1996:15–21.
2. Ishii S, Palmer AK, Werner FW, Short WH, Fortino MD. An anatomic study of the ligamentous structure of the triangular fibrocartilage complex. J Hand Surg 1998;23A:977–985.
3. Haugstvedt JR, Berger RA, Nakamura T, Neale P, Berglund L, An KN. Relative contributions of the ulnar attachments of the triangular fibrocartilage complex to the dynamic stability of the distal radioulnar joint. J Hand Surg 2006;31A:445–451.
4. Hagert CG. Distal radius fracture and the distal radioulnar joint: anatomical considerations. Handchir Mikrochir Plast Chir 1994;26: 22–26.
5. Trumble TE, Gilbert M, Vedder N. Isolated tears of the triangular fibrocartilage: management by early arthroscopic repair. J Hand Surg 1997;22A:57–65.
6. Hermansdorfer JD, Kleinman WB. Management of chronic peripheral tears of the triangular fibrocartilage complex. J Hand Surg 1991;16A:340–346.
7. Sennwald GR, Lauterburg M, Zdravkovic V. A new technique of reattachment after traumatic avulsion of the TFCC at its ulnar insertion. J Hand Surg 1995;20B:178–184.
8. Adams BD, Berger RA. An anatomic reconstruction of the distal

radioulnar ligaments for posttraumatic distal radioulnar joint instability. J Hand Surg 2002;27A:243–251.
9. Heiple KG, Freehafer AA, Van't Hof A. Isolated traumatic dislocation of the distal end of the ulna or distal radio-ulnar joint. J Bone Joint Surg 1962;44A:1387–1394.
10. Adams BD, Samani JE, Holley KA. Triangular fibrocartilage injury: a laboratory model. J Hand Surg 1996;21A:189–193.
11. Palmer AK. Triangular fibrocartilage complex lesions: a classification. J Hand Surg 1989;14A:594–606.
12. Yin Y, Mann FA, Hodge JC, Gilula LA. Roentgenographic interpretation of ligamentous instabilities of the wrist. In: Gilula LA, Yin Y, eds. Imaging of the wrist and hand. Philadelphia: WB Saunders, 1996:203–224.
13. Allieu Y, Garcia-Elias M. Dynamic radial translation instability of the carpus. J Hand Surg 2000;25B:33–37.
14. Goto A, Moritomo H, Murase T, Oka K, Sugamoto K, Arimura T, et al. In vivo three-dimensional wrist motion analysis using magnetic resonance imaging and volume-based registration. J Orthop Res 2005;23:750–756.
15. Crisco JJ, Coburn JC, Moore DC, Akelman E, Weiss AP, Wolfe SW. In vivo radiocarpal kinematics and the dart thrower's motion. J Bone Joint Surg 2005;87A:2729–2740.
16. Moritomo H, Murase T, Goto A, Oka K, Sugamoto K, Yoshikawa H. In vivo, three-dimensional kinematics of the midcarpal joint of the wrist. J Bone Joint Surg 2006;88A:611–621.
17. Marai GE, Laidlaw DH, Demiralp C, Andrews S, Grimm CM, Crisco JJ. Estimating joint contact areas and ligament lengths from bone kinematics and surfaces. IEEE Trans Biomed Eng 2004;51: 790–799.
18. Garcia-Elias M. Soft-tissue anatomy and relationships about the distal ulna. Hand Clin 1998;14:165–176.
19. Ritt MJ, Stuart PR, Berglund LJ, Linscheid RL, Cooney WP III, An KN. Rotational stability of the carpus relative to the forearm. J Hand Surg 1995;20A:305–311.
20. Weaver L, Tencer AF, Trumble TE. Tensions in the palmar ligaments of the wrist. I. The normal wrist. J Hand Surg 1994;19A:464–474.
21. Wiesner L, Rumelhart C, Pham E, Comtet JJ. Experimentally induced ulno-carpal instability: a study on 13 cadaver wrists. J Hand Surg 1996;21B:24–29.
22. Cooney WP, Linscheid RL, Dobyns JH. Triangular fibrocartilage tears. J Hand Surg 1994;19A:143–154.
23. Mikic ZD. Treatment of acute injuries of the triangular fibrocartilage complex associated with distal radioulnar joint instability. J Hand Surg 1995;20A:319–323.

SCIENTIFIC ARTICLE

Corrective Osteotomy for Malunited Intra-Articular Fracture of the Distal Radius Using a Custom-Made Surgical Guide Based on Three-Dimensional Computer Simulation: Case Report

Kunihiro Oka, MD, Hisao Moritomo, MD, Akira Goto, MD, Kazuomi Sugamoto, MD, Hideki Yoshikawa, MD, Tsuyoshi Murase, MD

We report a case of malunited intra-articular fracture of the distal radius successfully treated with corrective osteotomy through an extra-articular approach using a custom-made surgical guide that was designed based on preoperative three-dimensional computer simulation. *(J Hand Surg 2008;33A:835–840. Copyright © 2008 by the American Society for Surgery of the Hand. All rights reserved.)*

Key words: Computer simulation, corrective osteotomy, malunited intra-articular fracture, surgical guide.

MALUNITED INTRA-ARTICULAR FRACTURE of the distal radius may cause pain, restrict the range of motion, and result in osteoarthritis of the wrist joint.[1–7] Recently, several investigators have reported different techniques of intra-articular corrective osteotomy for symptomatic intra-articular malunion.[8–11] However, even with these techniques, it is still difficult to perform an accurate osteotomy through the original fracture line on the articular surface and reduce the malunited fragment to the correct position to reconstruct a smooth joint surface.[11] An operative procedure involving arthrotomy has the inherent risk of postoperative joint contracture.[8] The malunited fragment, if completely dissected from the parent radius, can become necrotic.[9,10] Less-invasive arthroscopic procedures require considerable surgical skills to accomplish an appropriate intra-articular corrective osteotomy. On the other hand, the recent progress in computed tomography (CT) imaging and computer technology has enabled us to simulate an accurate three-dimensional (3-D) corrective osteotomy using CT bone models. Furthermore, the development of an intraoperative guiding system that uses a custom-made surgical template makes it possible to perform an operation as simulated before the actual operation in spinal surgery,[12–14] joint arthroplasty,[15] and dental implantation.[16,17]

Here, we report a case of malunited intra-articular fracture of the distal radius that was successfully treated through an extra-articular approach using a simulation guidance system that consists of an original 3-D computer program and a custom-made surgical guide, which was designed to reproduce a preoperative simulation during the actual surgery.

From the Department of Orthopaedic Surgery, Osaka University Graduate School of Medicine, Osaka, Japan.

Received for publication December 21, 2007; accepted in revised form February 8, 2008.

This work was supported in part by the Japan Science and Technology Agency.

Corresponding author: Tsuyoshi Murase, MD, Department of Orthopaedic Surgery, Osaka University Graduate School of Medicine, 2-2, Yamada-oka, Suita, Osaka 565-0871, Japan; e-mail: tmurase-osk@umin.ac.jp.

0363-5023/08/33A06-0005$34.00/0
doi:10.1016/j.jhsa.2008.02.008

CASE REPORT

A 32-year-old man sustained a volar Barton fracture of the left distal radius and was initially treated by open reduction and internal fixation with a volar plate. The fracture united and the plate was removed 5 months after the operation; however, the patient complained of wrist pain and restriction of wrist motion. He was subsequently referred to our institution.

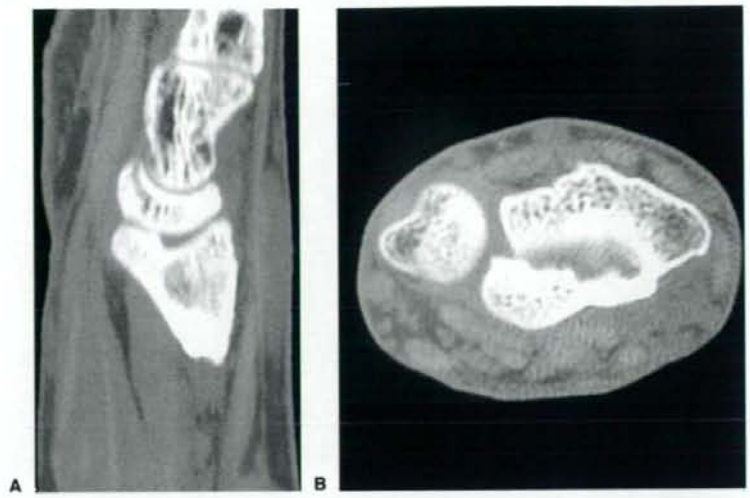

FIGURE 1: Computed tomography showed **A** a 3-mm step-off of the articular surface of the distal radius and **B** distal and ulnar migration of the volar fragment.

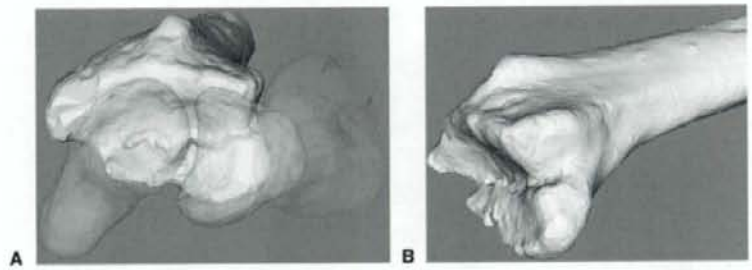

FIGURE 2: A, B A 3-D bone model of the radius indicates a malunion of the ulnovolar fragment of the distal radius.

On physical examination, wrist extension and flexion were restricted to 45° and 5°, respectively, with marked pain. Grip strength was 22 kg compared to 53 kg in the opposite hand. Radiographs revealed an irregular articular surface of the distal radius. CT showed a 3-mm articular step-off with distal migration of the fragment (Fig. 1).

Simulation

To plan corrective surgery for this intra-articular deformity of the distal radius, we attempted to simulate the 3-D correction of the deformity using computer models of the bones. First, the wrist was scanned by CT (scan time 0.5 s, slice thickness 0.625 mm, 10 mA, 120 kV; LightSpeed Ultra 16, General Electric, Waukesha, WI), and the digital data were entered in the computer. The contours of the radius, ulna, and proximal row of the carpal bones were semiautomatically segmented, and 3-D surface models were constructed based on the 3-D surface generation of the bone's cortex[18] using a VTK-based original computer program (Visualization Toolkit; Kitware Inc., Clifton Park, NY). Then, by deleting the bone marrow data, we obtained the complete surface models of the bones. The 3-D bone model of the radius showed a step-off at the articular surface of the distal radius with distal migration of the volar fragment (Fig. 2). In the computer simulation, the volar fragment was divided along the step-off and was reduced to the level of the original articular surface. The correction was completed by sliding the volar fragment 3 mm in the proximal direction (Fig. 3). To reproduce this simulation of intra-articular corrective osteotomy through an extra-articular approach, a customized surgical guide with multiple drilling holes to divide the malunited fragment was designed using commercially available software (Magics RP 10; Materialize, Leuven, Belgium) to exactly fit onto the volar surface of the distal

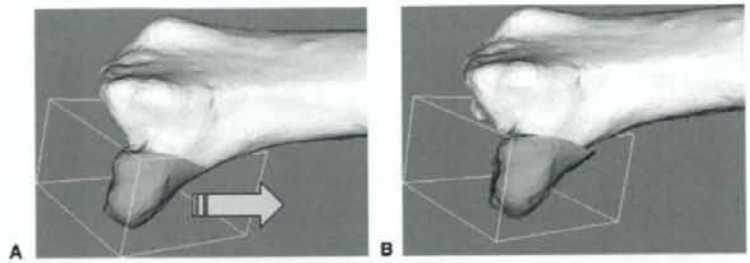

FIGURE 3: A, B Correction of the radius was accomplished by sliding the volar fragment 3 mm proximally.

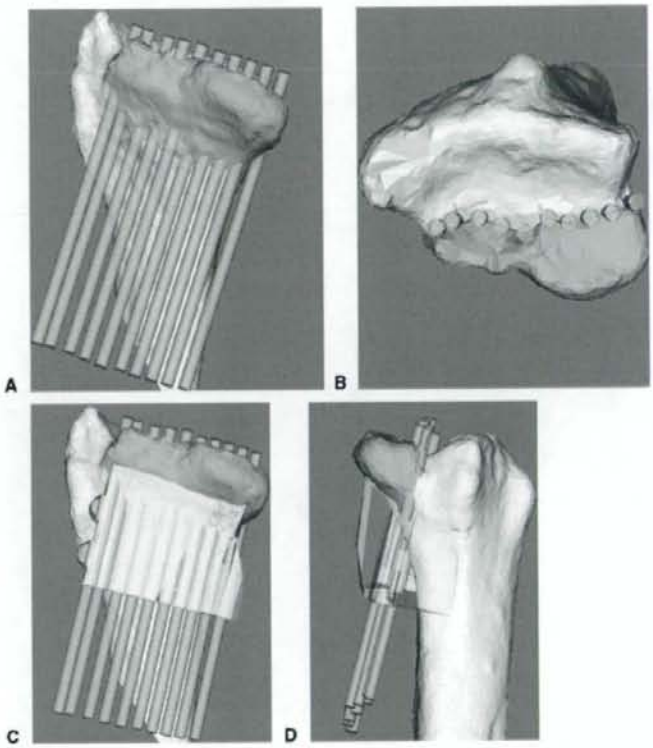

FIGURE 4: Computer planning of an intra-articular osteotomy. A, B Multiple wires (blue) were set along the deformity line to perform osteotomy. C, D A customized surgical guide (yellow), which fit on the bone surface and which was equipped with drill holes, was designed.

radius (Fig. 4). Then, the surgical guide was molded as a real plastic model with medical-grade resin in a rapid prototyping machine (Eden 250; Objet Geometries Ltd., Rehovot, Israel), which was accurate to within 30 μm. The guide was equipped with guide holes to set sleeves for K-wires. The diameter of the guide hole for a stainless drill sleeve, which had an internal diameter of 1.3 mm, was set at 3.0 mm. The surgical guide was sterilized with ethylene oxide (Fig. 5).

Surgical technique

The volar surface of the distal radius was exposed through a conventional volar approach, and the surgical guide was closely fit. K-wires (1.2 mm [0.047 in]) were passed through a drill sleeve while confirming penetration of the ends through the articular step-off under arthroscopic visualization (Fig. 6A, B). In total, 10 wires were placed, and an osteotomy was accomplished using a chisel along the borings (Fig. 6C). The fragment

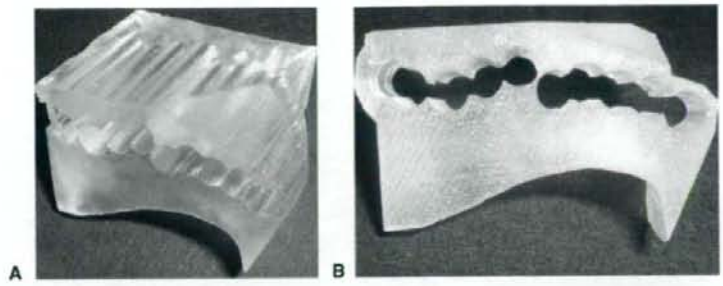

FIGURE 5: A, B The surgical guide was embodied as a real plastic model.

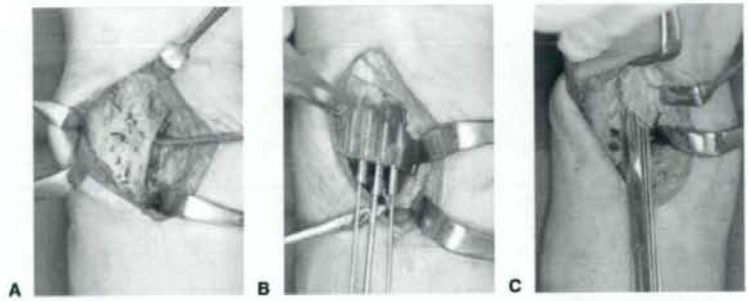

FIGURE 6: A The volar surface of the distal radius was exposed. B The surgical guide was fit, and K-wires were passed through drill sleeves under arthroscopic visualization. C The bone was divided using a chisel along the borings.

was completely separated from the radius with the volar radiocarpal ligaments attached to it. The fragment was moved proximally 3 mm and fixed temporally with 2 K-wires. After the reduction of the articular surface was confirmed with arthroscopy and an x-ray image intensifier, the fragment was fixed with 2 double-threaded screws (DTJ screw; Meira Co., Ltd., Nagoya, Japan), which have been shown to provide strong holding power for small bone fragments.[19]

Complete reduction of the step-off was achieved without arthrotomy, and a postoperative radiograph clearly showed that the incongruity of the radiocarpal joint was corrected. Cast immobilization was maintained for 3 weeks postoperatively. The patient was able to actively exercise the wrist and forearm, under the supervision of a physiotherapist, because good fixation between the fragment and the radius was achieved and wrist contracture after the intra-articular osteotomy was prevented. Three months after surgery, bone union had been achieved, the range of motion had improved, and the pain had disappeared. At the final follow-up 3 years after surgery, the congruity of the radiocarpal joint was preserved on radiographs (Fig. 7), and a smooth radial articular surface was observed on CT scans (Fig. 8). Wrist extension and flexion improved to 80° and 70°, respectively, and the grip strength increased from 22 kg preoperatively to 45 kg postoperatively. Furthermore, the patient no longer complained of any functional limitation in activities of daily living.

DISCUSSION

Incongruity of the wrist joint because of displaced intra-articular fragments is one of the major concerns after distal radius fractures.[2,4,7,20] Failure to reduce the articular surface to less than 2 mm of the step-off is considered to be a cause of posttraumatic osteoarthritis,[4,7,8,10] for which partial or total wrist arthrodesis has often been indicated.[21–25] Few studies have reported corrective osteotomies for intra-articular malunions of the distal radius, with and without arthroscopic assistance; however, these procedures are still associated with problems.[4,8,10,11] It is not always possible to adequately evaluate the complex 3-D intra-articular malunion with plain radiographs and intermittent slices of CT images. Consequently, the first problem that a surgeon encounters is planning an appropriate corrective surgery. In the actual surgery, it is not easy to perform an accurate osteotomy through a malunited fracture line from a limited field of view. Arthrotomy is usually performed from the dorsal side of the wrist joint to

FIGURE 7: Anatomic correction and congruity of the radiocarpal joint was obtained after surgery. **A** Anteroposterior and **B** lateral radiographs 3 years and 4 months after surgery are shown.

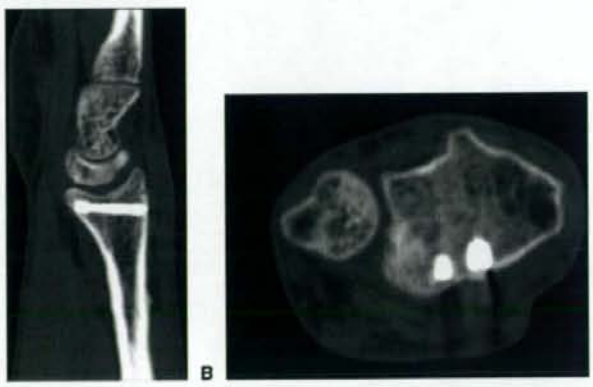

FIGURE 8: **A**, **B** Computed tomography shows congruity of the radiocarpal joint and complete obliteration of the step-off.

preserve the volar radiocarpal ligaments, which are the main stabilizers of the radiocarpal and midcarpal joints. Therefore, a malunited fragment located at the volar articular surface is difficult to operate on. Concerning postoperative wrist function, an open procedure of the wrist joint might lead to restricted range of joint motion due to fibrosis. Arthroscopic surgery is a less invasive alternative for managing intra-articular pathology. However, it is technically demanding to insert a targeting device into the tight volar joint space of the wrist, place it exactly on the fracture line, and perform an appropriate osteotomy under arthroscopic visualization.

We tried to perform an accurate intra-articular corrective osteotomy using 3-D computer simulation and a custom-made surgical guide. The advantage of the computer simulation is its ability to devise an accurate

operative plan with CT bone models. The customized surgical guide enabled us to realize the preoperative simulation of intra-articular corrective osteotomy through an extra-articular approach during the actual surgery. A CT-based, custom-made surgical guide has been reported to be used in spinal surgery techniques such as insertion of pedicle screws,[12–14] total joint arthroplasty for bone cutting,[15] and innominate osteotomy,[26] and this procedure has been confirmed as a practical method for implementation of computerized planning. Custom-made drill guides have also been commercially produced for performing dental implants.[17,18] We modified this technique for performing a corrective osteotomy of a malunited intra-articular fracture. By making multiple drill holes on the guide, we were able to perform an accurate osteotomy through the malunited fracture line on the articular surface through an extra-articular approach, just as preoperatively simulated. After the osteotomy was performed, the reduction could be completed simply by sliding the fragment proximally. Although arthroscopy was performed, it was only used to confirm that each step of the surgical procedure was done correctly.

The computer program described here is currently available only at our institution. Approximately 2 hours was required to complete the preoperative simulation, and the CT scanning and stereolithography modeling cost about $180 and $360, respectively. We believe that these shortcomings can be overcome with the advancement of technology and could well be offset by the above-mentioned advantages. This initial account of an intra-articular corrective osteotomy assisted by computer simulation and a custom-made surgical guide indicates that accurate and reliable anatomic reduction and an excellent clinical outcome can be achieved with this technique. We believe that our technique of computer simulation guidance is useful in planning and performing intra-articular corrective surgery through an extra-articular approach and hope that it will provide a novel treatment option for malunited intra-articular distal radius fractures.

REFERENCES

1. Fernandez DL, Geissler WB. Treatment of displaced articular fractures of the radius. J Hand Surg 1991;16A:375–384.
2. Trumble TE, Schmitt SR, Vedder NB. Factors affecting functional outcome of displaced intra-articular distal radius fractures. J Hand Surg 1994;19A:325–340.
3. Axelrod T, Paley D, Green J, McMurtry RY. Limited open reduction of the lunate facet in comminuted intra-articular fractures of the distal radius. J Hand Surg 1988;13A:372–377.
4. Bradway JK, Amadio PC, Cooney WP. Open reduction and internal fixation of displaced, comminuted intra-articular fractures of the distal end of the radius. J Bone Joint Surg 1989;71A:839–847.
5. Melone CP Jr. Open treatment for displaced articular fractures of the distal radius. Clin Orthop Relat Res 1986;202:103–111.
6. Szabo RM, Weber SC. Comminuted intraarticular fractures of the distal radius. Clin Orthop Relat Res 1988;230:39–48.
7. Knirk JL, Jupiter JB. Intra-articular fractures of the distal end of the radius in young adults. J Bone Joint Surg 1986;68A:647–659.
8. Gobel F, Vardakas DG, Riano F, Vogt MT, Sarris I, Sotereanos DG. Arthroscopically assisted intra-articular corrective osteotomy of a malunion of the distal radius. Am J Orthop 2004;33:275–277.
9. del Pinal F, Garcia-Bernal FJ, Delgado J, Sanmartin M, Regalado J, Cerezal L. Correction of malunited intra-articular distal radius fractures with an inside-out osteotomy technique. J Hand Surg 2006; 31A:1029–1034.
10. Ring D, Prommersberger KJ, Gonzalez del Pino J, Capomassi M, Slullitel M, Jupiter JB. Corrective osteotomy for intra-articular malunion of the distal part of the radius. J Bone Joint Surg 2005;87A:1503–1509.
11. Marx RG, Axelrod TS. Intraarticular osteotomy of distal radial malunions. Clin Orthop Relat Res 1996;327:152–157.
12. Goffin J, Van Brussel K, Martens K, Vander Sloten J, Van Audekercke R, Smet MH. Three-dimensional computed tomography-based, personalized drill guide for posterior cervical stabilization at C1-C2. Spine 2001;26:1343–1347.
13. Birnbaum K, Schkommodau E, Decker N, Prescher A, Klapper U, Radermacher K. Computer-assisted orthopedic surgery with individual templates and comparison to conventional operation method. Spine 2001;26:365–370.
14. Brown GA, Firoozbakhsh K, DeCoster TA, Reyna JR Jr, Moneim M. Rapid prototyping: the future of trauma surgery? J Bone Joint Surg 2003;85A(Suppl 4): 49–55.
15. Hafez MA, Chelule KL, Seedhom BB, Sherman KP. Computer-assisted total knee arthroplasty using patient-specific templating. Clin Orthop Relat Res 2006;444:184–192.
16. Garg AK. Surgical templates in implant dentistry. Dent Implantol Update 2006;17:41–44.
17. Sarment DP, Al-Shammari K, Kazor CE. Stereolithographic surgical templates for placement of dental implants in complex cases. Int J Periodontics Restorative Dent 2003;23:287–295.
18. Lorensen WE, Cline HE. Marching cubes: a high resolution 3D surface construction algorithm. Comput Graph 1987;21:163–169.
19. Tanaka J, Yanagida H, Oomukai T, Okuno T. A newly developed double thread screw for carpal scaphoid fracture. J Jpn Soc Surg Hand 2002;19:643–647.
20. Catalano LW III, Cole RJ, Gelberman RH, Evanoff BA, Gilula LA, Borrelli J Jr. Displaced intra-articular fractures of the distal aspect of the radius. Long-term results in young adults after open reduction and internal fixation. J Bone Joint Surg 1997;79A:1290–1302.
21. Rayan GM. Wrist arthrodesis. J Hand Surg 1986;11A:356–364.
22. Weiss AP, Hastings H II. Wrist arthrodesis for traumatic conditions: a study of plate and local bone graft application. J Hand Surg 1995;20A:50–56.
23. Richterman I, Weiss AP. Wrist fusion. Hand Clin 1997;13:681–687.
24. Nagy L. Salvage of post-traumatic arthritis following distal radius fracture. Hand Clin 2005;21:489–498.
25. Yajima H, Kobata Y, Shigematsu K, Kawamura K, Takakura Y. Radiocarpal arthrodesis for osteoarthritis following fractures of the distal radius. Hand Surg 2004;9:203–209.
26. Radermacher K, Portheine F, Anton M, Zimolong A, Kaspers G, Rau G, et al. Computer assisted orthopaedic surgery with image based individual templates. Clin Orthop Relat Res 1998;354:28–38.